

https://doi.org/10.1070/QEL16241

Selective laser ionisation of radionuclide ^{63}Ni

G.O. Tsvetkov, A.B. D'yachkov, A.A. Gorkunov, A.V. Labozin, S.M. Mironov, V.A. Firsov, V.Ya. Panchenko

Abstract. **We report a search for a scheme of selective laser stepwise ionisation of radionuclide ^{63}Ni by radiation of a dye laser pumped by a copper vapour laser. A three-stage scheme is found with ionisation through an autoionising state (AIS): $3d^84s^2\,{}^3F_4(E = 0) \rightarrow 3d^94p\,{}^1F^o_3(31030.99\ cm^{-1}) \rightarrow 3d^94d\,{}^2[7/2]_4(49322.56\ cm^{-1}) \rightarrow$ AIS(67707.61 cm^{-1}) which, by employing saturated radiation intensities provides the ionisation selectivity of above 1200 for ^{63}Ni.**

Keywords: *nickel, radionuclide ^{63}Ni, laser photoionisation, autoionisation, selectivity.*

1. Introduction

Presently, autonomous energy sources are being actively developed, which are based on the beta-voltaic effect with employment of radionuclide ^{63}Ni (a source of β-radiation with an average energy of 0.17 MeV and the half-decay period of 100 years) [1–5]. Such small autonomous sources of electrical energy (~1–10 μW) with a service life of above 30 years might provide many-year energy supply for microsystems in difficult-to-access places. Such microsystems are used in space-based objects, systems for distributed Earth monitoring, continuity testing sensors incorporated in buildings or road carpets, cardio- and neuro-stimulators in medicine, etc.

Natural nickel comprises five stable isotopes, namely, ^{58}Ni, ^{60}Ni, ^{61}Ni, ^{62}Ni and ^{64}Ni with the abundances of 68.07%, 26.22%, 1.14%, 3.63% and 0.93%, respectively. A known method for producing radionuclide ^{63}Ni is a three-operation procedure: obtaining the initial material enriched in ^{62}Ni by using centrifugal separation, irradiating it in a reactor and conversion to a volatile compound followed by enrichment in radioisotope ^{63}Ni [6, 7]. Under the condition of the target enrichment in ^{62}Ni to ~50%, the content of ^{63}Ni in a final product may reach 50%. A further increase in the target isotope concentration requires additional centrifuging; however, realisation of this process becomes technically difficult because of high radioactivity.

Employment of laser technology for isotope separation in an atomic vapour [atomic variant of laser isotope separation (AVLIS)] can substantially reduce the cost of this process because the main part of installation (a laser system) is mounted outside the radioactivity zone.

The AVLIS method is based on laser selective stepwise photoionisation of diluted vapours of some element by the radiation of two or more variable-wavelength lasers [8]. The wavelength of spectrally narrow laser radiation is matched with absorption lines of the target isotope and atoms are stepwise excited and photoionised. Produced photoions of the target isotope are extracted from the vapour flow to a collector by means of an electric field; the rest atoms remaining neutral continue motion along initial trajectories. Efficiency of target isotope separation is determined by 'large' isotopic shifts in the excitation spectrum of the element (exceeding the spectral linewidth of laser radiation and the Doppler broadening of the absorption line) and by the possibility of light saturation at each stage of the ionisation process (for reducing atom losses from intermediate levels due to spontaneous decay and, hence, making the maximal yield of photoions [9]). By the level of light power and spectral and frequency characteristics, the system of tunable dye lasers (DLs) pumped by a copper vapour laser (CVL) is one of the most efficient for AVLIS [10]). Thus, ionisation schemes for NiI were searched for taking into account the lasing spectra of efficient dyes (in the wavelength range λ = 530–645 nm) and second-harmonic spectra for DL radiation.

Isotopic shifts known from scientific literature include more than 30 transitions of NiI arc spectra [11, 12]. However, almost all lines (with λ = 330–391 nm) are outside the desired range. In [13–15], a number of schemes were suggested with ionisation of NiI through the autoionising states (AIS):

$3d^84s^2\,{}^3F_4 + h\nu(3145\ Å) \rightarrow 3d^84s4p\,{}^3G^o_3 + h\nu(3254\ Å) \rightarrow$ AIS [13],

$3d^94s\,{}^3D_3 + h\nu(3249\ Å) \rightarrow 3d^84s4p\,{}^3G^o_4 + h\nu(3150\ Å) \rightarrow$ AIS [13],

$3d^84s^2\,{}^3F_4 + h\nu(3232\ Å) \rightarrow 3d^84s4p\,{}^3G^o_5 + h\nu(3152\ Å) \rightarrow$ AIS [13],

$3d^94s\,{}^3D_3 + h\nu(3051\ Å) \rightarrow 3d^84s4p\,{}^3F^o_4 + h\nu(6111\ Å) \rightarrow 3d^94d\,{}^2[7/2]_4 + h\nu(7482\ Å) \rightarrow$ AIS [14],

$3d^94s\,{}^3D_3 + h\nu(2748\ Å) \rightarrow 3d^84s4p\,{}^1D^o_2 + h\nu(7866\ Å) \rightarrow 3d^94d\,{}^2[7/2]_3 + h\nu(7750\ Å) \rightarrow$ AIS [15].

It is very difficult to obtain DL radiation with the power sufficient to efficiently ionise macroscopic quantities of the target isotope in the spectral range of these transitions.

G.O. Tsvetkov, A.B. D'yachkov, A.A. Gorkunov, A.V. Labozin, S.M. Mironov, V.A. Firsov, V.Ya. Panchenko National Research Center 'Kurchatov Institute', pl. Akad. Kurchatova 1, 123182 Moscow, Russia; e-mail: glebtsvetkov@mail.ru

Received 20 October 2016; revision received 31 October 2016
Kvantovaya Elektronika **47** (1) 48–53 (2017)
Translated by N.A. Raspopov

The present work is devoted to a search for an efficient scheme of laser selective ionisation of nickel isotopes by DL radiation under CVL pumping. An installation for studying NiI spectra in the atomic vapour by the method of stepwise resonance ionisation is described in Section 2. In Section 3, measured isotopic shifts for lines of some transitions from the ground and intermediate levels are given for even isotopes of NiI, and the structure of first transitions for ^{61}Ni and ^{63}Ni is considered. Odd AISs with the energy E = 67503–68013 cm^{-1} exceeding the ionisation threshold are searched for. Based on the results obtained, we have chosen a three-step selective ionisation scheme: $3d^84s^2\,{}^3F_4$ ($E = 0$) → $3d^94p\,{}^1F^o_3$ (31030.99 cm^{-1}) → $3d^94d\,{}^2[7/2]_4$ (49322.56 cm^{-1}) → AIS (67707.61 cm^{-1}), and measured the saturation intensities for all excitation stages. In Section 4, results are presented for selective ionisation of ^{63}Ni performed by this scheme.

2. Experimental setup

2.1. Laser system

The laser setup comprising a DL pumped by radiation of a CVL and a separator complex has been developed and designed at the National Research Centre 'Kurchatov Institute' for studying laser isotope separation in atomic vapour [16].

The CVL [master oscillator (MO) – amplifier] is fabricated on the basis of self-heated [17, 18] copper vapour LT-40Cu oscillator and thyratron modulators (with the wavelengths of 510 and 578 nm, output power 35–40 W, pulse repetition rate 10 kHz, pulse duration $\Delta\tau_{FWHM} \approx 20$ ns). Each DL comprises a MO and an amplifier. Cavities of the MO utilise a diffraction grating operating in the regime of grazing incidence. An average power of single-mode generation at the MO output is 100–200 mW (the spectral linewidth is $\Delta\nu_{FWHM} \approx 100$ MHz, $\Delta\tau_{FWHM} \approx 15$–20 ns). In a DL amplifier, the power is increased to 4–8 W. The design of the MO cavity provides smooth (without mode hopping) wavelength scanning in the single-mode regime over the range of ~1 Å by varying a voltage across the piezoelectric cell in a folding mirror unit of the cavity. Scanning in a wider range (more than 100 Å) is performed by a stepper motor. The radiation wavelength of the DL is controlled by LM007 precision instruments (Laser 2000, GmbH), which provide the absolute measurement accuracy of ~0.0005 Å. If necessary, the instruments are used as etalons to actively stabilise the radiation wavelength of any DL. More detailed information about the DL one can find in [19]. Beams at the output from DL amplifiers are telescoped to a diameter of 5–12 mm, collimated and directed to a mass-spectrometer chamber. To adjust the beams spatially, semi-transparent and/or dichroic mirrors are used. Radiation pulses from all DLs are synchronised in time in a single beam; however, if necessary, those can be separated in time by tens of nanoseconds with the help of corresponding spatial delay lines.

The employment of efficient laser dyes PM556, PM567, PM597, SR640 and Cresyl Violet provides the operation spectral range for the laser system of 530–645 nm. For obtaining tunable radiation in the UV spectral range (pumping at λ = 578 nm, dye Cresyl Violet, the lasing wavelength range is 623–645 nm), the DL radiation was converted to the second harmonic (λ = 312–323 nm, the average power is of up to 1 W) in a nonlinear β-BBO crystal (of size 4 × 4 × 5 mm with the phase-matching angles $\theta = 39°$, $\varphi = 90°$).

2.2. Mass-spectrometer chamber

Spectroscopic investigations in narrow collimated atomic beams, in particular, by the method of resonance stepwise ionisation, are performed using an installation comprised of a vacuum chamber with a pump system, heat evaporator and quadruple MS-7302 mass-spectrometer. A system of diaphragms arranged above the evaporator allows one to form a narrow atomic beam (perpendicular to the laser beam) with an opening angle of 3° (the Doppler broadening of lines is ~100 MHz). The laser beam crosses the atomic beam directly in the ionisation chamber of the ion source of the quadruple mass-spectrometer. The zone of laser radiation interaction with the atomic vapour has a shape of cylinder with a length of 2 mm and diameter of 2 mm (determined by the size of a diaphragm placed on the beam propagation path prior to the interaction zone). The axes of atomic and laser beams and the ion-optical axis of the mass-spectrometer are mutually orthogonal. Ions are detected by a secondary-emission multiplier. Experimental data are accumulated in real time. Software realised in LabVIEW (National Instruments) records data from wavelength meters and laser radiation detectors; signals from secondary-emission multiplier and through an interface unit varies a control voltage on a piezoelectric element of the DL cavity folding mirror, thus tuning the laser wavelength. Data obtained are recorded, processed, and estimated in real time.

In experiments with stable NiI isotopes, natural metal nickel was used for evaporation. In experiments with radionuclide ^{63}Ni, metallic powder mixture of natural nickel with radionuclide from a ^{63}Ni source of β-radiation was used ('RITVERC' GmbH, Russia).

3. Choice of the photoionisation scheme

3.1. First stage

The NiI ground level $3d^84s^2\,{}^3F_4$ (energy $E = 0$) and lower metastable level $3d^94s\,{}^3D_3$ (E = 204.786 cm^{-1}) were used as the initial levels. Their relative population at the temperature of nickel evaporation ~1700 °C is 0.41 and 0.27, respectively. According to [20], there are approximately 10 transitions from the levels $^3F_4$ and $^3D_3$ with the wavelengths of 280–323 nm. The three transitions have been chosen for investigation, which correspond to various electron configuration changes:

$3d^84s^2\,{}^3F_4 \rightarrow 3d^84s4p\,{}^3G^o_3$ (λ = 314 nm),

$3d^94s\,{}^3D_3 \rightarrow 3d^84s4p\,{}^3G^o_3$ (λ = 317 nm),

$3d^84s^2\,{}^3F_4 \rightarrow 3d^94p\,{}^1F^o_3$ (λ = 322 nm).

The ionisation potential for NiI equals 7.64 eV (61600 cm^{-1}), which makes it possible to study the structure of first transitions by the two-stage scheme with ionisation to continuum using a single DL. In experiments, the mass filter of the quadruple mass-spectrometer was adjusted to transmission of the isotope photoions. The DL wavelength was scanned and the photoion current was recorded. An example of the photoion signal of ^{58}Ni obtained in scanning the DL wavelength near the wavelength of the resonance transition $3d^84s^2\,{}^3F_4$ →

$3d^94p\,^1F^o_3$ is presented in Fig. 1. For determining the 'centre' of each transition more exactly, experimental points were approximated by the Voigt profile using the PAW software from the CERN programme library [21]. In Table 1, measured isotopic shifts of transition frequencies are presented for even isotopes NiI.

Excitation selectivity, along with the values of isotopic shifts, is determined by a hyperfine structure (HFS) of the transition for isotopes with a nonzero nucleus spin I. In our case, $I = 3/2$ for ^{61}Ni and 1/2 for ^{63}Ni. For the chosen transitions, interaction constants are known only for lower levels of isotope ^{61}Ni [22]. It is not sufficient for calculating the HFS for transitions with a change in the total atomic momentum $\Delta F = 0, \pm 1$ between sublevels of hyperfine multipletes with $F = J + I, J + I - 1, \ldots, |J - I|$, where J is the total electron momentum of the atom. Hence, the HFS of the first three transitions was found experimentally (Fig. 2).

The HFS of the transitions $^3F_4 \rightarrow {}^3G^o_3$ and $^3D_3 \rightarrow {}^3G^o_3$ proved to be such (Fig. 2) that selective photoionisation of ^{63}Ni is only possible through weak lines with $\lambda = 3146.012$ and 3166.438 Å, respectively. The HFS of the transition $^3F_4 \rightarrow {}^1F^o_3$ of isotope ^{63}Ni comprises three transitions with a change in F: $3.5 \rightarrow 3.5, 4.5 \rightarrow 3.5$ and $3.5 \rightarrow 2.5$. Experimentally, only two lines have been detected at $\lambda = 3222.559$ and 3222.566 Å. Probably, the intensive peak of the photoion signal ^{63}Ni at $\lambda = 3222.566$ Å is formed by two hyperfine transitions with close frequencies. The frequency distance from this peak to nearest peaks of the isotopes ^{64}Ni and ^{62}Ni is 0.75 and 1.21 GHz, respectively. Hence, the transition

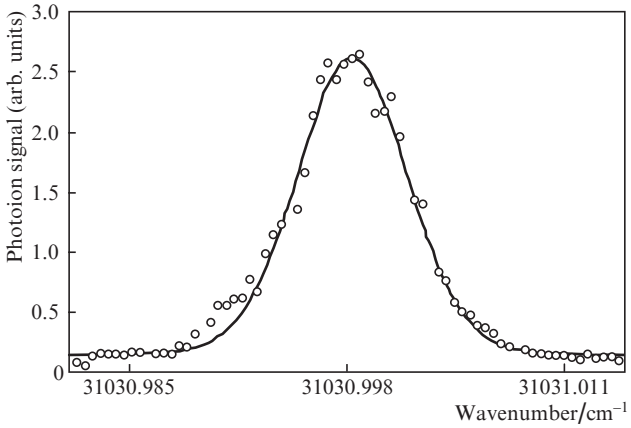

Figure 1. Photoion signal ^{58}Ni (dots) vs. DL radiation wavenumber of the first excitation stage ($3d^84s^2\,^3F_4 \rightarrow 3d^94p\,^1F^o_3$). The solid curve shows the Voigt profile with the Lorentz ($\Delta\nu_L$) and Gaussian ($\Delta\nu_D$) profile widths (FWHM) equal to 25 and 190 MHz, respectively.

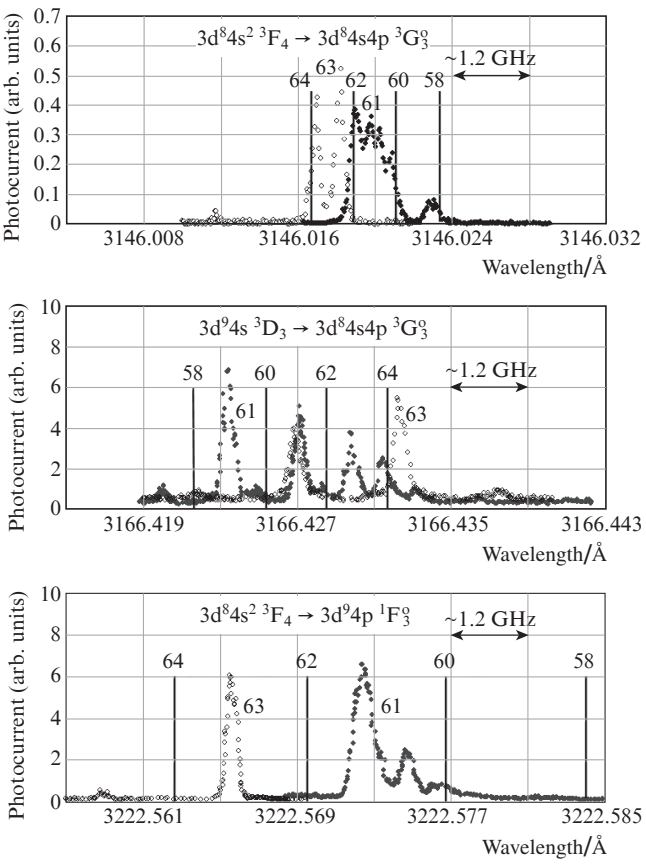

Figure 2. Isotopic structure of first transitions in NiI. Vertical lines denote the wavelengths of transitions for even NiI isotopes, points are HFS transitions of (•) ^{61}Ni and (o) ^{63}Ni.

$^3F_4 \rightarrow {}^1F^o_3$ was chosen as the first stage transition for the photoionisation scheme.

3.2. Second stage

Two-stage ionisation of nickel atoms can be performed through a set of known even AISs [13]; however, the tree-stage variant (one UV quantum and two visible-range quanta) is potentially preferable. First, selectivity of the two-step ionisation is lower because there is a channel of nonselective two-photon nonresonance ionisation. Second, the power of UV radiation at the output from a nonlinear β-BBO crystal is limited to the value of several watts due to a temperature dependence of the phase-matching angle [23, 24]. This may be insufficient for obtaining efficient ionisation. Transition from

Table 1. Isotopic shifts of transition frequencies for even isotopes NiI (the '–' sign means that the frequency for lighter isotope is higher).

Excitation stage	Transition	Wavelength*/Å	Isotopic shift/GHz			
			^{58}Ni–^{60}Ni	^{60}Ni–^{62}Ni	^{62}Ni–^{64}Ni	^{58}Ni–^{64}Ni
First	$3d^84s^2\,^3F_4 \rightarrow 3d^84s4p\,^3G^o_3$	3146.0237(3)	0.727(30)	0.728(30)	0.697(30)	2.152(30)
First	$3d^94s\,^3D_3 \rightarrow 3d^84s4p\,^3G^o_3$	3166.4219(3)	–1.077(30)	–0.928(30)	–0.957(30)	–2.962(30)
First	$3d^84s^2\,^3F_4 \rightarrow 3d^94p\,^1F^o_3$	3222.5841(3)	2.080(30)	2.080(30)	1.964(30)	6.124(30)
Second	$3d^94p\,^1F^o_3 \rightarrow 3d^94d\,^2[7/2]_4$	5464.0140(6)	0.423(15)	0.522(15)	0.504(15)	1.449(15)
Third	$3d^94d\,^2[7/2]_4 \rightarrow 67707.6$ cm^{-1}	5442.1623(6)	–1.641(30)	–1.419(30)	–2.055(30)	–5.115(30)

*The wavelength (vacuum) corresponds to transitions in ^{58}Ni.

the level $3d^94p\,{}^1F_3^o$ may occur to an even level with the total electron momentum J equal to 2, 3, or 4. In the spectral range of efficient DL generation, according to [20], transitions to the following levels are possible:

$3d^94d\,{}^2[7/2]_4$ (E = 49332.593 cm^{-1}, λ = 546 nm),

$3d^94d\,{}^2[7/2]_3$ (E = 49313.814 cm^{-1}, λ = 547 nm),

$3d^94d\,{}^2[3/2]_2$ (E = 49159.030 cm^{-1}, λ = 551nm),

$3d^84s5s\,{}^5F_4$ (E = 49085.982 cm^{-1}, λ = 554 nm).

For determining the wavelengths and isotopic shifts, the wavelength of DL radiation in the second stage (pumping at λ = 510 nm, the dye is PM556, the generation wavelength range is 530–550 nm, the density of the average power is 50 mW cm^{-2}) was scanned near the wavelength of the resonance transition; simultaneously, the first-stage DL (80 mW cm^{-2}) was stabilised at the wavelength of 3222.5841 Å. An additional DL (pumped at λ = 510 nm, the dye is PM556, the radiation wavelength is 535 nm, the density of the average power is 1 W cm^{-2}) was used for increasing the probability of ionising to continuum from the second level.

The search for second transitions we limited to studying the transition $3d^94p\,{}^1F_3^o \rightarrow 3d^94d\,{}^2[7/2]_4$, because, on the one hand, it has noticeable isotopy (Table 1); on the other hand, a very intensive autoionisation transition has been discovered from its upper level $3d^94d\,{}^2[7/2]_4$ (see below).

3.3. Third stage (autoionisation)

While using the DL pumped by radiation of the CVL, the fourth level (AIS) in the ionisation scheme should have an energy in the range of 64663–68189 cm^{-1} and be odd with the total electron momentum J = 1–5 depending on the third (pre-ionisation) level. According to [14], in the range E = 62577–67157 cm^{-1} only one odd AIS with the energy of 62694 cm^{-1} and J = 3 was found. Our laser system slightly expanded the search range. The wavelength of third-stage DL radiation (excitation from the level $3d^94d\,{}^2[7/2]_4$, E = 49332.593 cm^{-1}) was scanned in the lasing range of PM556 dye: λ = 535–550 nm (E = 67503–68013 cm^{-1}). Seven AISs have been found in the scanning (Table 2). While ionising through the most intensive autoionision transition (E_{AIS} = 67707.611 cm^{-1}) (Fig. 3), the photoion signal exceeded the signal of photoionisation to continuum by a factor of 630. For determining the total electron momentum J of this AIS we

Table 2. AIS of ^{58}Ni excited in transitions from the level $3d^94d\,{}^2[7/2]_4$ (E = 49332.561 cm^{-1}).

Transition wavelength (in vacuum)/Å	Transition line width (FWHM)/GHz	AIS energy/ cm^{-1}	K
5460.293	18	67646.598	3.2
5456.925	0.4	67657.903	5.5
5452.601	0.6	67672.431	11
5442.162	**1.1**	**67707.611**	**630**
5435.736	30	67729.336	4.5
5428.130	0.2	67755.112	11.5
5424.010	12.3	67769.105	5.7

Notes: K is the ratio of the current of photoionisation through the AIS to the current of photoionisation to continuum at the average radiation power density of 1 W cm^{-2}.

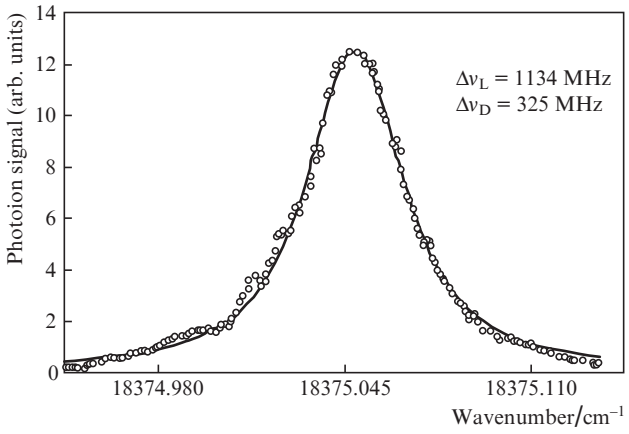

Figure 3. Photoion signal of ^{58}Ni during ionisation through the AIS with E_{AIS} = 67707.611 cm^{-1} vs. the wavenumber of the third-stage DL (excitation from the level $3d^94d\,{}^2[7/2]_4$, E = 49332.561 cm^{-1}).

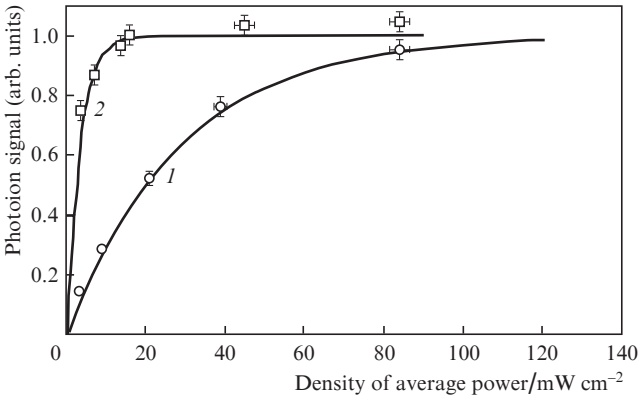

Figure 4. Dependences of the photoion signal on the average power density of the first-stage DL (the average power densities of the second- and third-stage DLs are 80 mW cm^{-2} and 1 W cm^{-2}, respectively) (*1*) and of the second-stage DL (the average power densities of the first- and third-stage DLs are 80 mW cm^{-2} and 1 W cm^{-2}, respectively) (*2*).

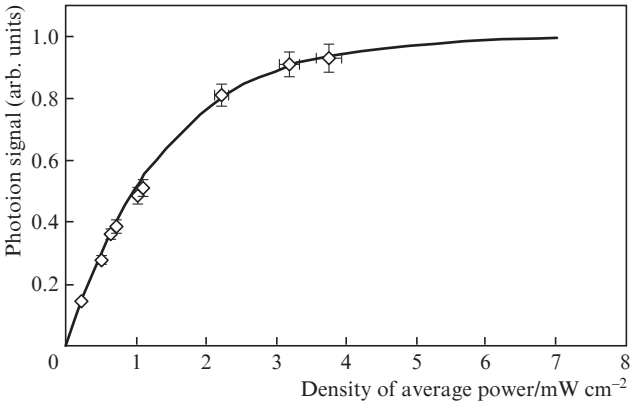

Figure 5. Dependence of the photoion signal on the average power density of the third-stage DL (the average power densities of the first- and second-stage DLs are 80 and 15 mW cm^{-2}, respectively).

experimentally studied the possibility of ionising through this state using another pre-ionisation level with E = 67707.611 cm^{-1} from the configuration $3d^94d\,{}^2[7/2]_3$ with J = 3. Ionisation has not been observed in the experiment; hence, one may assume

that the total electron momentum for the AIS with E_{AIS} = 67707.611 cm^{-1} is equal to 5.

The most important characteristic of any photoionisation scheme is the intensity of laser radiation needed for each stage to provide saturation of the transition. From this one can estimate the photoionisation efficiency at prescribed laser powers and expenses of the required efficiency for the separation process. To find these characteristics, we experimentally studied dependences of the photoion signal on the average laser power density. These dependences are shown in Figs 4 and 5 for all excitation stages. The saturation levels for the first, second, and third stages are 80, 15 and 4000 mW cm^{-2}, respectively. The final scheme of three-stage ionisation of NiI is presented in Fig. 6.

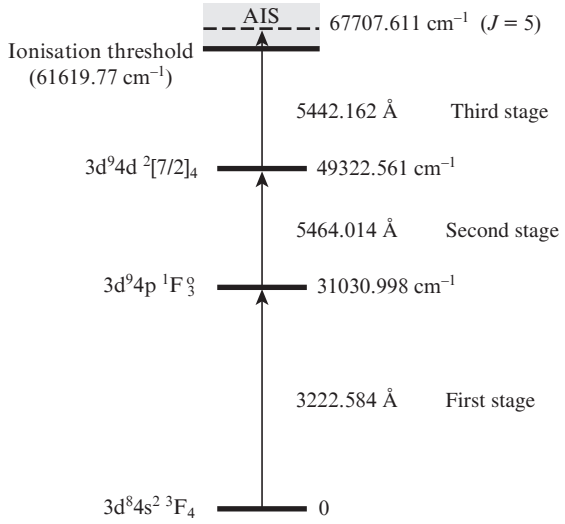

Figure 6. Three-stage scheme of ionising NiI through the AIS. Level energies and wavelengths (vacuum) correspond to ^{58}Ni.

4. Selective photoionisation

The wavelengths of lasers for selective photoionisation of the radionuclide were adjusted in several steps. First, the mass filter of the quadruple mass-spectrometer was adjusted to transmission of ions with the mass of 63. The first-stage DL was adjusted to the wavelength of the most intensive component of the ^{63}Ni spectrum (λ_1 = 3222.5656 Å) and was switched into the regime of automatic wavelength stabilisation. Then, the wavelengths of the second- and third-stage DLs were successively adjusted to the maximal photocurrent of radionuclide ^{63}Ni (λ_2 = 5464.0058 Å, λ_3 = 5442.1953 Å) and were also stabilised. For determining selectivity of ^{63}Ni photoionisation, the mass-spectrometer was scanned in the mass number range of 57–65. An example mass-spectrum of the photoion signal is presented in Fig. 7. In experiment, the densities of the average DL power of the first, second and third stages were 80, 15 and 1700 mW cm^{-2}, respectively, and were close to the saturation levels (Figs 4 and 5).

The concentration of ^{63}Ni ions in the photoion current (at the radionuclide initial concentration of less than 1%) was 93%. In Table 3, results of experiments on selective ionisation of various low-abundance isotopes NiI are given. One can see that photoionisation selectivity for ^{61}Ni is lower than, e.g., for ^{63}Ni. Seemingly, this is related with that the lines of ^{61}Ni in the

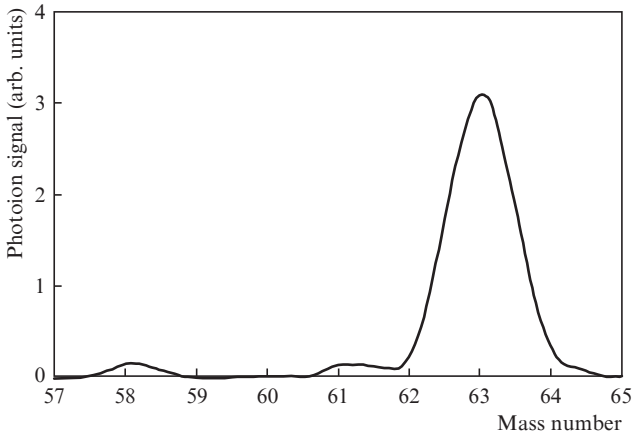

Figure 7. Mass-spectrum of photoions. The initial isotope concentration of ^{63}Ni was less than 1%, the average power densities of DLs of the first, second and third stages are 80, 15 and 1700 mW cm^{-2}, respectively.

spectrum are close to the lines of even isotopes with a comparatively high concentration, namely, ^{60}Ni (26.22%) and ^{62}Ni (3.63%). In addition, if the wavelength of the first-stage DL is adjusted to a HFS component of ^{63}Ni, then a greater part of atoms is involved into the process of photoexcitation with following photoionisation because the ground state of ^{63}Ni is split into only two sublevels, whereas atoms ^{61}Ni in the ground state are distributed over four sublevels.

Table 3. Selectivity S of laser ionisation for isotopes NiI at the saturated radiation intensities according to the scheme 3d^{8}4s^2 ^{3}F$_4$ → 3d^{9}4p ^{1}F$^o_3$ → 3d^{9}4d ^{2}[7/2]$_4$ → AIS (67707.611 cm^{-1}).

Isotope	C_f	C_p	S
^{61}Ni	0.011	0.75	265
^{62}Ni	0.036	>0.98	>1300
^{63}Ni	<0.01	0.93	>1200
^{64}Ni	0.009	>0.98	>5000

Note: $S = C_p(1 - C_f)/[C_f(1 - C_p)]$, where C_f is the initial concentration of the target isotope and C_p is the concentration of photoions of the target isotope.

5. Conclusions

Experiments on atomic nickel spectroscopy performed by the method of resonance stepwise ionisation allowed us to find an efficient scheme for selective ionisation of isotopes NiI by radiation of a DL pumped by a CVL: 3d^{8}4s^2 ^{3}F$_4$ (E = 0) → 3d^{9}4p ^{1}F$^o_3$ (31030.99 cm^{-1}) → 3d^{9}4d ^{2}[7/2]$_4$ (49322.56 cm^{-1}) → AIS (67707.61 cm^{-1}). Selectivity of radionuclide ^{63}Ni separation obtained in the experiments at relatively weak requirements on power output characteristics of the laser system allows us to consider the method of laser isotope separation in atomic vapour (AVLIS) as quite promising for producing macro-quantities of radionuclide ^{63}Ni, which is a basis for designing long-service-life autonomous sources of electrical energy.

Acknowledgements. The work was supported by the Russian Foundation for Basic Research (Grant No. 16-29-09459-ofi-m).

References

1. Nagornov Yu.S. *Sovremennye aspekty primeneniya betavolaicheskogo effekta* (Modern Aspects of Betavoltaic Effect Applications) (Ul'yanovsk: UlGPU, 2012).
2. Pustovalov A.A., Gusev V.V., Zadde V.V., Petrenko N.S., Tikhomirov A.V., Tsvetkov L.A. *At. Energiya*, **103**, 353 (2007).
3. Pchelintseva E.S. *Cand. Thesis* (Ul'yanovsk, Udmurt State Univ., 2011).
4. Reznev A.A., Pustovalov A.A., et al. *Nano- i Mikrosistemnaya Tekhnika*, **3**, 14 (2009).
5. http://www.findpatent.ru/patent/245/2452060.html.
6. Sosnin L.J., Suvorov I.A., Tcheltsov A.N., Rogozev B.I., Gudov V.I. *Nucl. Instrum. Methods Phys. Res., Sect. A*, **334**, 43 (1993).
7. http://www.findpatent.ru/patent/231/2313149.html.
8. Ambartsumyan R.V., Kalinin V.P., Letokhov V.S. *Pis'ma Zh. Exp. Teor. Fiz.*, **13**, 305 (1971).
9. Letokhov V.S., Mishin V.I., Puretskii A.A., in *Khimiya plazmy* (Plasma Chemistry) (Moscow: Atomizdat, 1977) Vol. 4, p. 3.
10. Bass I.L., Bonanno R.E., Hackel R.P., Hammond P.R. *Appl. Opt.*, **33**, 6993 (1992).
11. Schroeder D.J., Mack J.E. *Phys. Rev.*, **121**, 1726 (1961).
12. Steudel A. *Z. Phys. A: At. Nucl.*, **296**, 189 (1980).
13. Lievens P. *Phys. Rev. A*, **54**, 2253 (1996).
14. Jokinen A. *Nucl. Instrum. Methods Phys. Res., Sect. B*, **126**, 95 (1997).
15. Kessler T. *J. Phys. B: At. Mol. Opt. Phys.*, **40**, 4413 (2007).
16. Babichev A.P. et al. *Kvantovaya Electron.*, **35**, 879 (2005) [*Quantum Electron.*, **35**, 879 (2005)].
17. Isaev A.A., Kazaryan M.A., Petrash G.G. *Pis'ma Zh. Exp. Teor. Fiz.*, **16**, 40 (1972).
18. Belyaev V.P., Zubov V.V., Isaev A.A., et al. *Kvantovaya Electron.*, **12**, 74 (1985) [*Sov. J. Quantum Electron.*, **15**, 40 (1985)].
19. Grigoriev I., Diachkov A., Kuznetzov V., Labosin V., Firsov V. *Proc. SPIE Int. Soc. Opt. Eng.*, **5121**, 411 (2003).
20. http://grotrian.nsu.ru.
21. http://cernlib.web.cern.ch/cernlib/.
22. Childs W.J., Goodman L.S. *Phys. Rev.*, **170**, 136 (1968).
23. Yap Y.K. *Opt. Lett.*, **23**, 1016 (1998).
24. Takahashi M. *Jpn. J. Appl. Phys.*, **49**, 080211 (2010).